A Compound with Coexisting Mono- and Dinuclear Cu(II) Complexes Hosting a New Water Tape Cluster $(H_2O)_{22}$

Wei Xu and Yue-Qing Zheng

Center of Applied Solid State Chemistry Research, Ningbo University, Ningbo, 315211, P. R. China

Reprint requests to Prof. Dr. Yue-Qing Zheng. Fax: Int. +574/87600747.
E-mail: yqzhengmc@163.com

Z. Naturforsch. **2014**, *69b*, 987 – 994 / DOI: 10.5560/ZNB.2014-4156
Received July 12, 2014

A new compound containing mono- and dinuclear Cu(II) complexes, $[Cu_2(phen)_2(H_2O)_2(OH)_2][Cu(phen)_2(CO_3)]_2(HCO_3)_2 \cdot 22H_2O$ (phen = 1,10-phenanthroline), has been prepared and characterized by X-ray diffraction analysis, thermoanalytical techniques and temperature-dependent magnetic susceptibility measurements. The hydroxo-bridged dinuclear $[Cu_2(phen)_2(H_2O)_2(OH)_2]^{2+}$ complex cations and the mononuclear $[Cu(phen)_2(CO_3)]$ complex molecules are assembled *via* $\pi\cdots\pi$ stacking interactions into layers. A novel water tape containing $(H_2O)_{22}$ cluster units has been observed in the structure of the title complex. In hydrogen bond interactions HCO_3^- anions act as donor and acceptor to link the water tapes to form an infinite 2D network parallel to (010). According to the magnetic analyses, the coupling interactions in the dinuclear complex cation is ferromagnetic ($J = 34.5\ cm^{-1}$).

Key words: Copper(II) Complex, Hydroxo-bridging, Water Cluster, Magnetic Properties, Supramolecular Assembly

Introduction

Special attention has been devoted to polynuclear assemblies of transition metal ions recently, which is directly related to the search for strategies to design new systems exhibiting desired physical and chemical properties [1 – 3]. Among them, polynuclear copper(II) clusters are of special interest not only due to the central role they play in biological systems but also for their magneto-structural correlations [4 – 9]. To build these molecular architectures, dinuclear motifs can be viewed as the basic building units to form multinuclear systems such as, *e. g.*, with the hydroxo-bridged planar $[Cu(\mu_y\text{-}OH)_2Cu]$ core [5]. In the presence of bidentate chelating 1,10-phenanthroline (phen) ligands, the Cu atoms in the $[Cu(\mu_y\text{-}OH)_2Cu]$ core are able to accommodate a fifth ligand (X) to complete a square-pyramidal coordination, forming centrosymmetric dinuclear $[Cu_2(phen)_2(OH)_2(H_2O)_2]^{2+}$ complex cations [10 – 13]. The two hydroxo-bridged dinuclear copper(II) complexes $[Cu_2(phen)_2(OH)_2(H_2O)_2]$ and $[Cu_2(phen)_2(OH)_2X_2]$ (X = $HCOO^-$, HCO_3^- and CO_3^{2-}) have also been explored by several other investigators [14 – 17]. However, compounds with coexisting mono- and dinuclear copper(II) complexes have been rarely studied [18].

Water clusters, groups of lattice water molecules held together by hydrogen bonds, are believed to be a perfect model connecting isolated water molecules to bulk water. The structures of crystal hosts offer attractive environments for stabilizing various topologies of water clusters, which play important roles in the formation of different water morphologies [19 – 23]. To obtain 1D water morphologies, it is important to construct host frameworks suitable for water molecules extending into chains or tapes. Chen *et al*. have pointed out that the planar molecular complexes $[M_2L_2]$ (L = 2,2′-bipyridine-like ligands) may serve as effective building blocks for the construction of various 2D supramolecular arrays for the stabilization of water morphologies [24]. However, the relationship between the host structure and the water clusters is somehow difficult to delineate. Moreover, it is difficult to find a general principle of the stabilization of water arrays. Therefore, gaining different water motifs in closely related host structures can provide a better understanding of the rel-

ative importance of the various weak interactions that are responsible for their stabilization.

We present here a novel 1D water morphology for a $(H_2O)_{22}$ subunit embedded in the structure of a Cu(II) compound $[Cu_2(phen)_2(H_2O)_2(OH)_2][Cu(phen)_2(CO_3)]_2(HCO_3)_2{\cdot}22H_2O$, which was characterized by single-crystal X-ray diffraction, IR spectroscopy, TG and elemental analysis, and temperature-dependent magnetic measurements. To the best of our knowledge, the title compound represents a rare example consisting of both hydroxo-bridged dinuclear $[Cu_2(phen)_2(H_2O)_2(OH)_2]^{2+}$ complex cations and mononuclear $[Cu(phen)_2(CO_3)]$ complex molecules.

Results and Discussion

Syntheses

Previous work has shown that Cu(II) ions and 1,10-phenanthroline react with CO_3^{2-} ions to give $[Cu(phen)_2CO_3]{\cdot}7H_2O$ by hydrothermal synthetic procedures at room temperature [25 – 30]. In the presence of succinic acid, self-assembly of Cu(II) ions, 1,10-phenanthroline and CO_3^{2-} ions in CH_3OH/H_2O at pH = 10 resulted in the title complex $[Cu_2(phen)_2(H_2O)_2(OH)_2][Cu(phen)_2(CO_3)]_2(HCO_3)_2 \cdot 22H_2O$ which consists of hydroxo-bridged dinuclear $[Cu_2(phen)_2(H_2O)_2(OH)_2]^{2+}$ complex cations and $[Cu(phen)_2(CO_3)]$ complex molecules, while the corresponding reactions at weakly acidic or neutral pH values yielded two succinato-bridged Cu(II) coordination polymers $[Cu(phen)(C_4H_4O_4)]_2{\cdot}C_4H_6O_4$ [31] and $[Cu(phen)(C_4H_4O_4)]_2{\cdot}2H_2O$ [32], respectively. Clearly, a higher pH value is advantageous for the formation of the dinuclear $[Cu(OH)_2Cu]^{2+}$ core and reduces the ability of the succinato ligand to coordinate with Cu(II) ions.

Description of the crystal structure

The title complex consists of centrosymmetric dinuclear $[Cu_2(phen)_2(H_2O)_2(OH)_2]^{2+}$ complex cations, mononuclear $[Cu(phen)_2(CO_3)]$ complex molecules, HCO_3^- anions, and water molecules. As shown in Fig. 1, within the $[Cu_2(phen)_2(H_2O)_2(OH)_2]^{2+}$ complex cations, the metal atoms are each coordinated by a phenanthroline ligand, two μ_2-OH^- ions and an apical aqua ligand to complete a distorted square-pyramidal CuN_2O_3 coordination sphere. The Cu–N

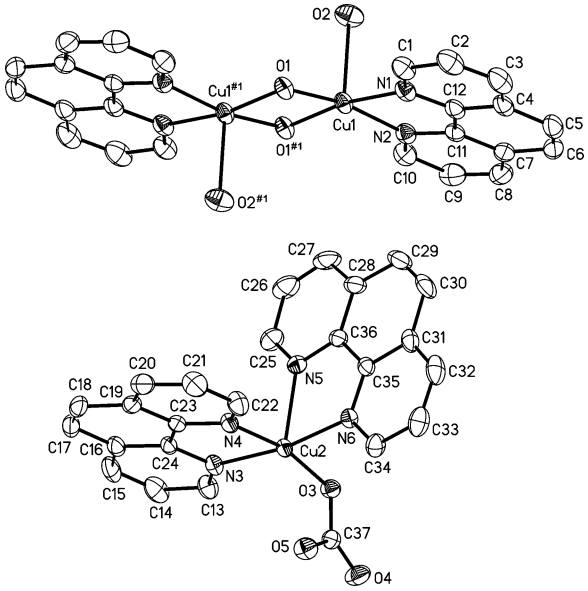

Fig. 1. ORTEP view of the structure of components of the title complex (40 % probability displacement ellipsoids). Symmetry transformations used to generate equivalent atoms: #1 = $-x+1, -y, -z+1$.

bond lengths are in range of 2.006(3) – 2.037(3) Å (Table 1), while the equatorial and axial Cu–O bond lengths are 1.940(2) and 2.250(3) Å, respectively. The Cu atom exhibits a deviation of 0.194(1) Å from the basal plane defined by the N atoms and the hydroxo O atoms towards the apical aqua ligand. The $[Cu(phen)_2(CO_3)]$ complex molecule shows close similarity to those found in $[Cu(phen)_2(CO_3)]{\cdot}7H_2O$ [25] and $[Cu(phen)_2(HCO_3)]ClO_4$ [33]. Within the present complex molecule, the metal atom adopts a significantly distorted octahedral coordination geometry defined by four N atoms of two chelating phenanthroline ligands and two O atoms of one chelating carbonate anion with the Cu–N distances in the region 2.028(3) – 2.264(3) Å, and Cu–O distances of 1.944(2) and 2.519(3) Å. The chelating ligands around the Cu atom are orientated approximately perpendicular to each other with a dihedral angle of 89.63(4)°.

The phenanthroline ligands present in different units of the compound display nearly perfect coplanarity. Along the crystallographic *a* axis the dinuclear $[Cu_2(phen)_2(H_2O)_2(OH)_2]^{2+}$ complex cations are arranged in such a way that adjacent phenanthroline ligands of different cations are engaged in intercationic face-to-face $\pi\cdots\pi$ stacking interactions with

Table 1. Selected bond lengths (Å), angles (deg) and hydrogen bonding contacts (Å, deg) for the title complex with estimated standard deviations in parentheses [a].

Distances			
Cu1–O1	1.938(2)	Cu2–O3	1.944(2)
Cu1–O1$^{\#1}$	1.945(2)	Cu2–N3	2.029(3)
Cu1–O2	2.252(3)	Cu2–N4	2.030(3)
Cu1–N1	2.037(3)	Cu2–N5	2.264(3)
Cu1–N2	2.007(3)	Cu2–N6	2.028(3)
Angles			
O1–Cu1–O1$^{\#1}$	83.3(1)	O3–Cu2–N3	93.7(1)
O1–Cu1–O2	95.1(1)	O3–Cu2–N4	166.6(1)
O1–Cu1–N1	96.1(1)	O3–Cu2–N5	96.2(1)
O1–Cu1–N2	167.7(1)	O3–Cu2–N6	93.6(1)
O1$^{\#1}$–Cu1–O2	97.9(1)	N3–Cu2–N4	81.6(1)
O1$^{\#1}$–Cu1–N1	169.7(1)	N3–Cu2–N5	94.7(1)
O1$^{\#1}$–Cu1–N2	97.0(1)	N3–Cu2–N6	170.5(1)
O2–Cu1–N1	92.4(1)	N4–Cu2–N5	96.7(1)
O2–Cu1–N2	97.1(1)	N4–Cu2–N6	92.8(1)
N1–Cu1–N2	81.4(1)	N5–Cu2–N6	78.3(1)

Hydrogen bonding contacts

D–H	*d*(D–H)	*d*(H···A)	*d*(D–H···A)	∠(D–H···A)	A
O1–H1A	0.85	2.00	2.842(6)	172	O7
O2–H2A	0.85	1.90	2.740(5)	168	O5
O2–H2B	0.85	1.87	2.705(5)	169	O8
O6–H6A	0.85	1.91	2.760(5)	180	O13
O9–H9A	0.86	2.07	2.902(6)	161	O10$^{\#2}$
O9–H9B	0.87	1.98	2.842(6)	172	O7
O10–H10A	0.86	2.10	2.881(6)	151	O8
O10–H10B	0.86	2.01	2.803(5)	152	O14
O11–H11A	0.80	2.31	2.797(5)	120	O18$^{\#3}$
O11–H11B	0.80	2.54	3.223(6)	146	O4$^{\#4}$
O11–H11B	0.79	2.59	3.143(6)	129	O12
O12–H12A	0.84	1.92	2.740(5)	166	O4$^{\#4}$
O12–H12B	0.81	2.12	2.893(6)	160	O9$^{\#2}$
O13–H13A	0.83	2.01	2.820(5)	163	O14
O13–H13B	0.88	1.93	2.778(5)	162	O15
O14–H14A	0.85	1.90	2.744(5)	169	O16
O14–H14B	0.88	1.92	2.762(5)	160	O11
O15–H15A	0.84	1.99	2.812(5)	169	O17
O15–H15B	0.85	1.94	2.790(5)	177	O12$^{\#5}$
O16–H16A	0.89	1.87	2.754(5)	172	O5$^{\#4}$
O16–H16B	0.82	2.05	2.843(6)	163	O1$^{\#2}$
O17–H17A	0.81	2.00	2.778(5)	163	O19$^{\#6}$
O17–H17B	0.84	2.10	2.871(6)	152	O19$^{\#3}$
O18–H18A	0.83	1.89	2.722(5)	173	O3
O19–H19A	0.81	1.93	2.710(5)	161	O4
O19–H19B	0.83	2.04	2.781(5)	148	O18

[a] Symmetry transformations used to generate equivalent atoms: #1 $= -x+1, -y, -z+1$; #2 $= -x+1, -y+1, -z+1$; #3 $= -x+1, -y+1, -z$; #4 $= x, y+1, z$; #5 $= x-1, y, z$; #6 $= x-1, y+1, z$.

a mean interplanar distance of 3.41 Å. Obviously, such interactions are responsible for the supramolecular assembly of the dinuclear cations into positively charged chains parallel to [100]. On the other hand, the complex molecules are aligned in the [100] direction so that each N5-containing phenanthroline ligand is sandwiched by two symmetry-related partners with the mean interplanar distances alternatively at

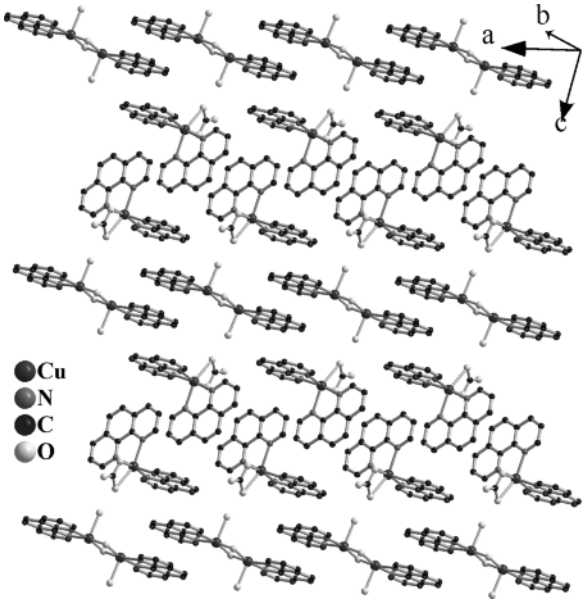

Fig. 2. The layers extending parallel to (010) in the structure of the title complex.

3.38 and 3.42 Å, suggesting again significant intermolecular $\pi\cdots\pi$ stacking interactions, due to which the complex molecules are assembled to generate columnar neutral chains with the N3-containing phenanthroline ligands being orientated outwards. Moreover, the phenanthroline ligands of the dinuclear complex cations are observed to be involved in $\pi\cdots\pi$ stacking interactions to the N3-donor ligands (the mean interplanar distance is 3.31 Å). Apparently, such $\pi\cdots\pi$ stacking interactions between the cationic and neutral chains are a driving force to form supramolecular layers parallel to (010), as demonstrated in Fig. 2. The cationic layers are found to be stabilized by hydrogen bonds between aqua ligands in the dinuclear complex cations and the carbonato oxygen atoms of the mononuclear complex molecules. The hydroxo-bridged dinuclear $[Cu_2(phen)_2(H_2O)_2(OH)_2]^{2+}$ complex cations are assembled into cationic layers due to $\pi\cdots\pi$ stacking interactions between adjacent *N*-donor ligands. The $[Cu(phen)_2(CO_3)]$ complex molecules in $[Cu(phen)_2(CO_3)]\cdot 7H_2O$ are also supramolecularly assembled to generate corrugated layers on the basis on the $\pi\cdots\pi$ stacking interactions [26]. From this viewpoint, the cationic layers present in the title complex could be visualized as an admixture from synergetic assemblage of the $[Cu_2(phen)_2(H_2O)_2(OH)_2]^{2+}$ complex cations and the $[Cu(phen)_2(CO_3)]$ complex molecules.

Many complexes containing $[Cu_2(phen)_2(H_2O)_2(OH)_2]^{2+}$ cations have been reported in previous work [10 – 18]. In these compounds, the counteranions are inorganic, organic and complex anions. A large variety of water clusters, such as $(H_2O)_2$, $(H_2O)_4$, $(H_2O)_5$, $(H_2O)_6$, $(H_2O)_{10}$ and T4(0)6(0), have also been observed in these crystalline hydrates.

In the title compound there are eleven crystal water molecules in the asymmetric unit (from O9 to O19) forming a $(H_2O)_{22}$ cluster associated by O–H···O hydrogen bonds. The geometrical parameters pertaining to the water cluster are collected in Table 1. Within the water cluster, the O···O distances are in the range of 2.744 – 3.143 Å with an average distance of 2.834 Å, which is slightly longer than the value of 2.759 Å in ice I_h at −90 °C [34], but it is very close to that observed in liquid water (2.854 Å) [35]. As shown in Fig. 3, not every O atom in the cluster shows four-coordination. The eleven water molecules form five-membered and seven-membered rings sharing one edge (O11, O14). The $(H_2O)_{11}$ subunit has one dangling water molecule (O16) pointing away from the rings. Through O17···O19 hydrogen bonding, the $(H_2O)_{11}$ subunit is connected with an equivalent related by a crystallographic inversion center forming a $(H_2O)_{22}$ water cluster with one four-membered ring, two five-membered rings and two seven-membered rings. To the best of our knowledge, such a structure of a $(H_2O)_{22}$ water cluster has not been reported so far. Adjacent $(H_2O)_{22}$ cluster units are assembled by O12···O15 hydrogen bonds into extended water tapes along [100]. Between adjacent water tapes, HCO_3^- anions act as donors and acceptors to link the tapes to form an infinite 2D network parallel to (010). The water molecules and the HCO_3^- anions are located between the cationic supramolecular layers. The layers are pillared to produce an infinite supramolecular edifice (Fig. 4). In this sense, the water layer is different from reported water clusters and other morphologies, which are situated in host cavities or channels generated by metal-organic coordination moieties.

Thermal analysis

Thermal analysis (Fig. 5) has shown that the title complex decomposes in several small steps. Between 60 – 150 °C the TG curve witnesses a first weight

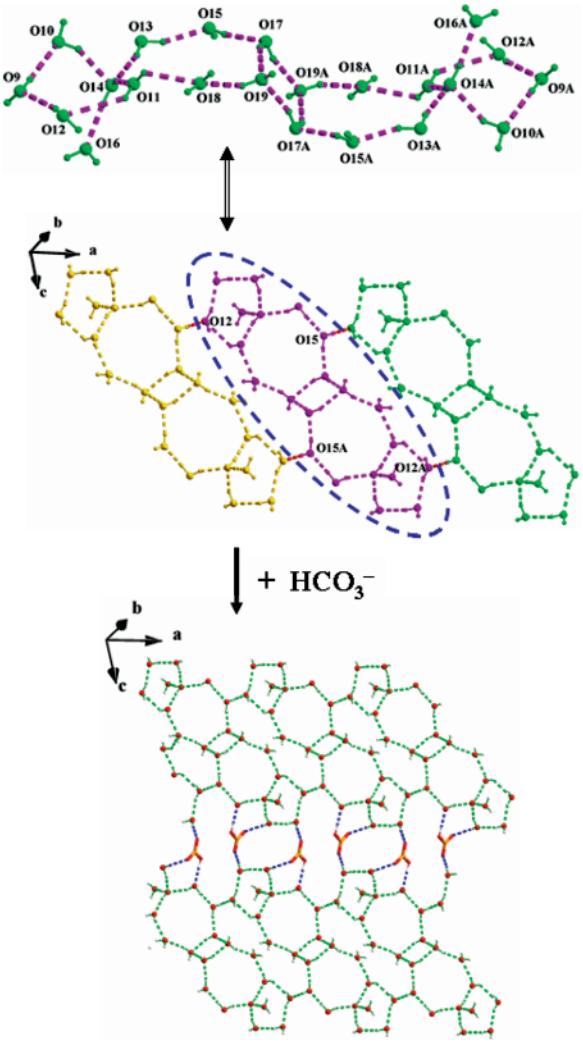

Fig. 3 (color online). The 1D water tape containing $(H_2O)_{22}$ units in the structure of the title complex.

loss of 22 %, corresponding to the value of 23 % calculated for the removal of 26 mol water molecules (22 water molecules, 2 aqua ligands and 2 water molecules resulting from OH^- anions). The residue is assumed to be an intermediate tentatively formulated as "$[Cu(phen)(CO_3)][Cu(phen)_2(CO_3)]$". The weight loss of 45 % between 200 – 408 °C can be attributed to the decomposition of the intermediate accompanied by liberation of CO_2 and phenanthroline ligands. Upon further heating, the sample gradually loses additional weight, and the final black remnant amounts to 31 % at 700 °C.

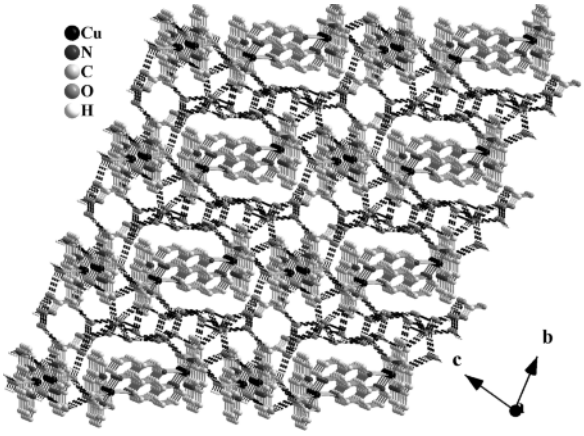

Fig. 4. Overall crystal structure of the title complex.

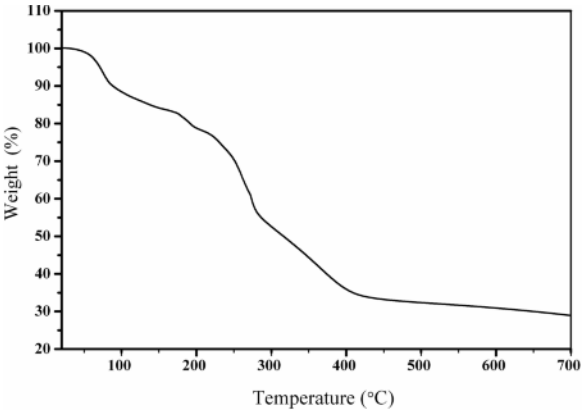

Fig. 5. TG curve for the title complex.

Magnetic properties

The magnetic susceptibility of powdered samples of the title compound was measured as a function of temperature over 2 – 300 K in a fixed magnetic field of 5000 Oe. The effective magnetic moment μ_{eff}gt room temperature is 3.81 μ_B, slightly larger than the value of 3.46 μ_B for four quasi-isolated Cu(II) ions ($S = 1/2$). When the temperature is lowered from room temperature, the μ_{eff} value first rises steadily to 4.3 μ_B at 6.4 K, revealing an overall ferromagnetic coupling between the magnetic centers, and then decreases rapidly, which may be due to zero field splitting effects. According to the structural description as presented above, the magnetic susceptibilities of the title complex result from mutual contribution from the centrosymmetric dinuclear $[Cu_2(phen)_2(H_2O)_2(OH)_2]^{2+}$

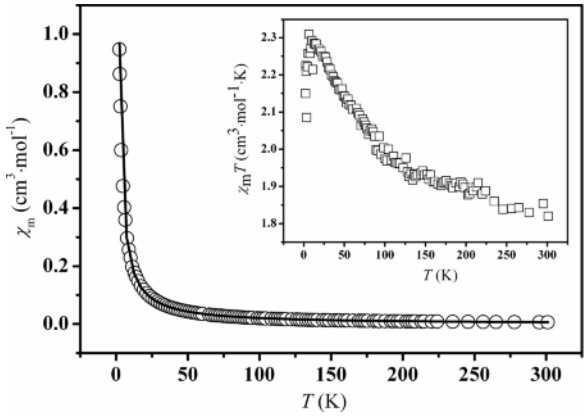

Fig. 6. Temperature dependence of the magnetic susceptibility of title complex. The solid line represents the best fit.

complex cation and the $[Cu(phen)_2(CO_3)]$ complex molecule, and therefore, the analysis of the magnetic behavior can be modelled by the following equation (on assumption $g_{di} = g_{mono} = g$):

$$\chi_M = \frac{2N\beta^2 g_{di}^2}{kT}[3 + \exp(-2J/kT)]^{-1} + \frac{N\beta^2 g_{mono}^2}{2kT} \quad (1)$$

N, g and β are Avogadro's number, g factor and Bohr magneton, respectively, and k is Boltzman's constant. The best fit is obtained with $g = 2.24$, $J = 34.5\,cm^{-1}$, $R = 2 \times 10^{-5}$ ($R = \Sigma(\chi_{obsd} - \chi_{calcd})^2/\Sigma\chi_{obsd}^2$), suggesting a ferromagnetic interaction between the Cu ions in the $[Cu_2(phen)_2(H_2O)_2(OH)_2]^{2+}$ complex cations (Fig. 6). This J value of $34.5\,cm^{-1}$ is very close to the value of $35.2\,cm^{-1}$ calculated from the empirical formula $2J = -74.53\theta + 7270$ ($\theta = 96.6(1)^\circ$ for the title complex) proposed by Hatfield *et al.* [36].

Conclusion

In summary, we have presented the preparation and properties of a compound containing hydroxo-bridged dinuclear together with a mononuclear copper(II) complexes, with 1,10-phenanthroline as the common ligand. The magnetic studies revealed an intradimer ferromagnetic interaction ($J = 34.5\,cm^{-1}$). The crystal structure analysis shows the coexistence of hydroxo-bridged dinuclear $[Cu_2(phen)_2(H_2O)_2(OH)_2]^{2+}$ complex cations and mononuclear $[Cu(phen)_2(CO_3)]$ complex molecules, held together by $\pi\cdots\pi$ stacking interactions into layers. The crystals host a novel water tape consisting of $(H_2O)_{22}$ water clusters which contain one four-membered ring, two five-membered rings and two seven-membered rings. This mode of a water structure has not been predicted theoretically, nor was it previously found experimentally. These new structural data will enhance the understanding of the structural aspects of water.

Experimental Section

Materials and physical methods

All chemicals of reagent grade were commercially available and used without further purification. Single-crystal X-ray diffraction data were collected by a Rigaku R-Axis Rapid X-ray diffractometer. The powder X-ray diffraction measurement was carried out with a Bruker D8 Focus X-ray diffractometer to check the phase purity. The C, H, N, and S microanalysis was performed with a Perkin Elmer 2400II CHNO/S elemental analyzer. The FT-IR spectrum was recorded from KBr pellets in the range $4000 - 400\,cm^{-1}$ on a Shimadzu FTIR-8900 spectrometer. Thermogravimetric measurements were carried out from r. t. to 700 °C on preweighed samples in an N_2 stream using a Seiko Exstar 6300 TG/DTA apparatus with a heating rate of $10\,°C\,min^{-1}$. The temperature-dependent magnetic susceptibility was determined with a Quantum Design SQUID magnetometer (Quantum Design Model MPMS-7) in the temperature range 2 – 300 K with an applied field of 5 kOe (1 kOe = $7.96 \times 10^4\,A\,m^{-1}$).

Synthesis of $[Cu_2(phen)_2(H_2O)_2(OH)_2][Cu(phen)_2(CO_3)]_2(HCO_3)_2 \cdot 22H_2O$

0.171 g (1.0 mmol) $CuCl_2 \cdot 2H_2O$, 0.198 g (1.0 mmol) 1,10-phenanthroline monohydrate and 0.118 g (1.0 mmol) succinic acid were subsequently added to 50 mL CH_3OH/H_2O (1 : 1, v/v). The mixture was stirred for 30 min and then filtered. The blue filtrate was adjusted to pH = 10.0 with $1\,mol\,L^{-1}$ Na_2CO_3 to give a dark-blue solution, which was then allowed to stand at room temperature. After several days, dark-blue plate-like crystals were obtained (yield: 30 % based on the $CuCl_2 \cdot 2H_2O$ input). The phase purity of the crystalline product was checked by comparing an experimental powder X-ray diffraction (PXRD) pattern with the one simulated on the basis of the single-crystal data (Fig. 7), as well as by an elemental analysis. – Anal. for $C_{76}H_{100}Cu_4N_{12}O_{38}$ (%): calcd. C 44.66, H 4.89, N 8.22; found C 44.54, H 4.95, N 8.18. – IR (KBr pellet, cm^{-1}): ν = 3385 vs, 3059 vw, 1624 vs, 1587 m, 1517 vs, 1496 m, 1427 s, 1338 s, 1256 m, 1144 m, 1105 m, 997 m, 864 s, 849 s, 725s, 646 m, 474 m, 428 m.

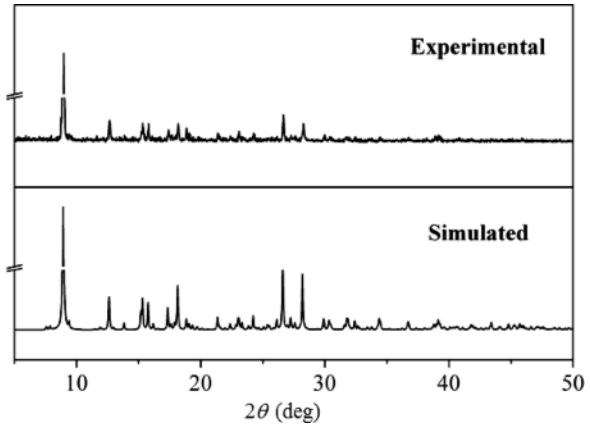

Fig. 7. Experimental and simulated PXRD patterns.

X-Ray structure determination

A suitable single crystal was selected under a polarizing microscope and fixed with epoxy cement on a fine glass fiber, which was then mounted on a Rigaku R-Axis Rapid IP X-ray diffractometer with graphite-monochromatized MoK_α radiation ($\lambda = 0.71073$ Å) for cell determination and subsequent data collection. The data were corrected for Lp and absorption effects. The SHELXS-97 and SHELXL-97 programs were used for structure solution and refinement, respectively [37 – 39]. The structure was solved by using Direct Methods, and all non-hydrogen atoms were located in subsequent difference Fourier syntheses. After several cycles of refinement, all hydrogen atoms associated with carbon atoms were geometrically generated, and the rest of the hydrogen atoms were located from the successive difference Fourier syntheses. Finally, all non-hydrogen atoms were refined with anisotropic displacement parameters by full-matrix least-squares techniques and hydrogen atoms with isotropic displacement parameters set to 1.2 or 1.5 times of the values for the associated heavier atoms. Detailed information about the crystal data and structure determination is summarized in Table 2. Selected interatomic distances and bond angles are tabulated in Table 1.

Table 2. Crystal structure data for the title complex.

Empirical formula	$C_{76}H_{100}Cu_4N_{12}O_{38}$
M_r	2043.88
Crystal size, mm^3	$0.38 \times 0.29 \times 0.25$
Crystal system	Triclinic
Space group	$P\bar{1}$ (no. 2)
a, Å	10.137(2)
b, Å	12.441(3)
c, Å	19.319(4)
α, deg	74.73(3)
β, deg	81.00(3)
γ, deg	71.30(3)
V, Å^3	2219(1)
Z	1
$D_{calcd.}$, g cm^{-3}	1.53
μ(MoK_α), mm^{-1}	1.0
F(000), e	1060
hkl range	$-13 \le h \le 1$; $-15 \le k \le 15$; $-25 \le l \le 25$
$((\sin\theta)/\lambda)_{max}$, Å^{-1}	0.65
Refl. measured / unique / R_{int}	11819/7262/0.0231
Param. refined	589
$R(F)/wR(F^2)$	0.0489/0.1235
GoF (F^2)[a]	1.022
$\Delta\rho_{fin}$ (max/min), e Å^{-3}	0.76/−0.52

CCDC 725662 contains the supplementary crystallographic data for this paper. These data can be obtained free of charge from The Cambridge Crystallographic Data Centre *via* www.ccdc.cam.ac.uk/data_request/cif.

Acknowledgement

This project was supported by the Open Foundation from Application of Nonlinear Science and Technology in the Most Important Subject of Zhejiang (grant no. xkzl2006). Honest thanks are also extended to the K. C. Wong Magna Fund in Ningbo University.

[1] M. O'Keeffe, O. M. Yaghi, *Chem. Rev.* **2012**, *112*, 675 – 702.
[2] S. A. K. Robinson, M. V. L. Mempin, A. J. Cairns, K. T. Holman, *J. Am. Chem. Soc.* **2011**, *133*, 1634 – 1637.
[3] M. D. Ward, *Chem. Commun.* **2009**, 4487 – 4499.
[4] P. E. Kruger, G. D. Fallon, B. Moubaraki, K. J. Berry, K. S. Murray, *Inorg. Chem.* **1995**, *34*, 4808 – 4814.
[5] X. Li, D. Y. Cheng, J. L. Lin, Z. F. Li, Y. Q. Zheng, *Cryst. Growth & Des.* **2008**, *8*, 2853 – 2861.
[6] W. Plass, *Coord. Chem. Rev.* **2009**, *253*, 2286 – 2295.
[7] C. J. Calzado, *Chem. Eur. J.* **2013**, *19*, 1254 – 1261.
[8] A. B. Caballero, A. Rodriguez-Dieguez, I. Vidal, *Dalton Trans.* **2012**, 1755 – 1764.
[9] S. Youngme, N. Wannarit, T. Remsungnen, N. Chaichit, G. A. van Albada, J. Reedijk, *Inorg. Chem. Commun.* **2008**, *11*, 179 – 185.
[10] L. P. Lu, S. D. Qin, P. Yang, M. L. Zhu, *Acta Crystallogr.* **2004**, *E60*, m950–m952.

[11] Y. Q. Zheng, J. Sun, J. L. Lin, *Z. Anorg. Allg. Chem.* **2000**, *626*, 613 – 615.
[12] Y. Q. Zheng, J. Sun, J. L. Lin, *Z. Kristallogr. NCS* **2000**, *215*, 533 – 534.
[13] G. R. Maldonado, M. Quirós, J. M. Salas, *Inorg. Chem. Commun.* **2010**, *13*, 399 – 403.
[14] Y. H. Sun, Y. J. Yi, H. L. Gao, J. Z. Cui, *Chinese J. Inorg. Chem.* **2008**, *24*, 161 – 164.
[15] Z. L. You, W. S. Liu, H. L. Zhu, H. K. Fun, *Trans. Metal Chem.* **2005**, *30*, 1 – 4.
[16] S. Iglesias, O. Castillo, A. Luque, P. Román, *Inorg. Chim. Acta* **2003**, *349*, 273 – 278.
[17] Y. Q. Zheng, J. L. Lin, J. Sun, *Z. Anorg. Allg. Chem.* **2001**, *627*, 1647 – 1651.
[18] Y. M. Jiang, J. L. Zeng, K. B. Yu, *Acta Crystallogr.* **2004**, *C60*, m543–m545.
[19] M. A. Saeed, A. Pramanik, B. M. Wong, *Chem. Commun.* **2012**, 8631 – 8633.
[20] W. Xu, H. L. Zhu, J. L. Lin, Y. Q. Zheng, *J. Coord. Chem.* **2013**, *66*, 171 – 179.
[21] R. Natarajan, J. P. H. Charmant, A. G. Orpen, A. P. Davis, *Angew. Chem. Int. Ed.* **2010**, *49*, 5125 – 5129.
[22] S. K. Ghosh, J. Ribas, M. S. E. Fallah, P. K. Bharadwaj, *Inorg. Chem.* **2005**, *44*, 3856 – 3862.
[23] D. Sun, H. R. Xu, C. F. Yang, Z. H. Wei, N. Zhang, R. B. Huang, L. S. Zheng, *Cryst. Growth Des.* **2010**, *10*, 4642 – 4649.
[24] J. P. Zhang, Y. Y. Lin, X. C. Huang, X. M. Chen, *Inorg. Chem.* **2005**, *44*, 3146 – 3150.
[25] Z. W. Mao, F. W. Heinemann, G. Liehr, R. van Eldik, *J. Chem. Soc., Dalton Trans.* **2001**, 3652 – 3662.
[26] R. P. Doyle, M. Nieuwenhuyzen, P. E. Kruger, *CrystEngComm* **2006**, *8*, 904 – 908.
[27] C. H. Zhou, L. J. Zhou, L. Tang, Y. Y. Wang, *Chin. Chem. Lett.* **2009**, *20*, 861 – 864.
[28] C. H. Zhou, L. J. Zhou, Z. L. Zhang, Y. Y. Wang, *J. Cluster Sci.* **2008**, *19*, 675 – 683.
[29] H. Korpi, P. J. Figiel, E. Lankinen, P. Ryan, M. Leskela, T. Repo, *Eur. J. Inorg. Chem.* **2007**, 2465 – 2471.
[30] Y. Q. Zheng, Z. P. Kong, J. L. Lin, *Z. Kristallogr. NCS* **2002**, *217*, 333 – 334.
[31] Y. Q. Zheng, J. Sun, J. L. Lin, *Z. Anorg. Allg. Chem.* **2000**, *626*, 1501 – 1504.
[32] Y. Q. Zheng, J. Sun, J. L. Lin, *Acta Chim. Sinica* **2000**, *58*, 1131 – 1135.
[33] Z. W. Mao, G. Liehr, R. van Eldik, *J. Am. Chem. Soc.* **2000**, *122*, 4839 – 4840.
[34] W. F. Kuhs, M. S. Lehman, *J. Phys. Chem.* **1983**, *87*, 4312 – 4313.
[35] A. H. Narten, W. E. Thiessen, L. Blum, *Science* **1982**, *217*, 1033 – 1034.
[36] V. H. Crawford, H. W. Richardson, J. R. Wasson, D. J. Hodgson, W. E. Hatfield, *Inorg. Chem.* **1976**, *15*, 2107 – 2110.
[37] G. M. Sheldrick, SHELXS-97, Program for the Solution of Crystal Structures, University of Göttingen, Göttingen (Germany), **1997**.
[38] G. M. Sheldrick, SHELXL-97, Program for the Solution of Crystal Structures, University of Göttingen, Göttingen (Germany) **1997**.
[39] G. M. Sheldrick, *Acta Crystallogr.* **2008**, *A64*, 112 – 122.